arXiv:1608.02880v1 [math.AP] 9 Aug 2016

INVERSE RANDOM SOURCE SCATTERING FOR ELASTIC WAVES

GANG BAO *, CHUCHU CHEN †, AND PEIJUN LI ‡

Abstract. This paper is concerned with the direct and inverse random source scattering problems for elastic waves where the source is assumed to be driven by an additive white noise. Given the source, the direct problem is to determine the displacement of the random wave field. The inverse problem is to reconstruct the mean and variance of the random source from the boundary measurement of the wave field at multiple frequencies. The direct problem is shown to have a unique mild solution by using a constructive proof. Based on the explicit mild solution, Fredholm integral equations of the first kind are deduced for the inverse problem. The regularized Kaczmarz method is presented to solve the ill-posed integral equations. Numerical experiments are included to demonstrate the effectiveness of the proposed method.

Key words. Inverse source scattering problem, elastic wave equation, stochastic partial differential equation, Fredholm integral equation

AMS subject classifications. 78A46, 65C30

1. Introduction.

The inverse source scattering problems, an important research subject in inverse scattering theory, are to determine the unknown sources that generate prescribed radiated wave pattens [13,23]. These problems are largely motivated by applications in medical imaging [19]. A typical example is to use electric or magnetic measurements on the surface of the human body, such as head, to infer the source currents inside the body, such as the brain, that produce the measured data. Mathematically, the inverse source scattering problems have been widely examined for acoustic and electromagnetic waves by many researchers [1–3, 8, 9, 15, 17, 29, 32]. For instance, it is known that the inverse source problem does not have a unique solution at a fixed frequency due to the existence of non-radiating sources [16, 21]; it is ill-posed as small variations in the measured data can lead to huge errors in the reconstructions [7].

Although the deterministic counterparts have been well studied, little is known for the stochastic inverse problems due to uncertainties, which are widely introduced to the models for two common reasons: randomness may directly appear in the studied systems [18, 20] and incomplete knowledge of the systems must be modeled by uncertainties [24]. A uniqueness result may be found in [14], where it showed that the auto-correlation function of the random source was uniquely determined everywhere outside the source region by the auto-correlation function of the radiated field. Recently, one-dimensional stochastic inverse source problems have been considered in [6, 10, 27], where the governing equations are stochastic ordinary differential equations. Utilizing the Green functions, the authors have presented the first approach in [5] for solving the inverse random source scattering problem in higher dimensions, where the stochastic partial differential equations are considered.

In this paper, we study both the direct and inverse random source scattering

*School of Mathematical Sciences, Zhejiang University, Hangzhou 310027, China; The research was supported in part by a Key Project of the Major Research Plan of NSFC (No. 91130004), an NSFC A3 Project (No.11421110002), NSFC Tianyuan Projects (No. 11426235; No. 11526211), and a special research grant from Zhejiang University. (baog@zju.edu.cn)

†Department of Mathematics, Michigan State University, East Lansing, MI 48824, USA. (chen2095@math.purdue.edu)

‡Department of Mathematics, Purdue University, West Lafayette, Indiana 47907, USA. This author's research was supported in part by the NSF grant DMS-1151308. (lipeijun@math.purdue.edu)

problems for elastic waves. Given the source, the direct problem is to determine the displacement of the random wave field. The inverse problem is to reconstruct the mean and variance of the random source from the boundary measurement of the wave field. Recently, the elastic wave scattering problems have received ever increasing attention for their significant applications in many scientific areas such as geophysics and seismology [11, 26, 28]. For example, they have played an important role in the problem for elastic pulse transmission and reflection through the Earth when investigating earthquakes and determining their focus, which is exactly the motivation of this work.

The random source is assumed to be driven by a white noise, which can be thought as the derivative of a Brownian sheet or a multi-parameter Brownian motion. The goal is to determine the mean and variance of the random source function by using the same statistics of the displacement of the wave field, which are measured on a boundary enclosing the compactly supported source at multiple frequencies. By constructing a sequence of regular processes approximating the rough white noise, we show that there exists a unique mild solution to the stochastic direct scattering problem. By studying the expectation and variance of the solution, we deduce Fredholm integral equations of the first kind for the inverse problem. It is known that Fredholm integral equations of the first kind are severely ill-posed, which can be clearly seen from the distribution of singular values for our integral equations. It is particularly true for the integral equations of reconstructing the variance. We present well conditioned integral equations via linear combination of the original equations. We propose a regularized Kaczmarz method to solve the resulting linear system of algebraic equations. This method is consistent with our multiple frequency data and requires solving a relatively small scale system at each iteration. Numerical experiments show that the proposed approach is effective to solve the problem.

This work is a nontrivial extension of the method proposed in [5] for the inverse random source scattering problem of the stochastic Helmholtz equation, to solve the inverse random source scattering problem of the stochastic Navier equation. Clearly, the elastic wave equation is more challenging due to the coexistence of compressional waves and shear waves that propagate at different speeds. The Green function is more complicated and has higher singularity for the Navier equation than that of the Helmholtz equation does. Hence more sophisticated analysis is required.

The paper is organized as follows. In section 2, we introduce the stochastic Navier equation for elastic waves and discuss the solutions of the deterministic and stochastic direct problems. Section 3 is devoted to the inverse problem, where Fredholm integral equations are deduced and the regularized Kaczmarz method is proposed to reconstruct the mean and the variance. Numerical experiments are presented in section 4 to illustrate the performance of the proposed method. The paper is concluded with general remarks in section 5.

2. Direct problem. In this section, we introduce the Navier equation for elastic waves and discuss the solutions of the deterministic and stochastic direct source scattering problems.

2.1. Problem formulation. Consider the scattering problem of the two-dimensional stochastic Navier equation in a homogeneous and isotropic medium

$$\mu\Delta\boldsymbol{u} + (\lambda+\mu)\nabla\nabla\cdot\boldsymbol{u} + \omega^2\boldsymbol{u} = \boldsymbol{f} \quad \text{in } \mathbb{R}^2, \tag{2.1}$$

where $\omega > 0$ is the angular frequency, λ and μ are the Lamé constants satisfying $\mu > 0$ and $\lambda + \mu > 0$, and $\boldsymbol{u} = (u_1, u_2)^\top$ is the displacement of the random wave field. As a

source, the electric current density $\boldsymbol{f} = (f_1, f_2)^\top$ is assumed to be a random function driven by an additive white noise and takes the form

$$\boldsymbol{f}(x) = \boldsymbol{g}(x) + \boldsymbol{h}(x)\dot{W}_x. \tag{2.2}$$

Here $\boldsymbol{g} = (g_1, g_2)^\top$ is a deterministic real vector function and $\boldsymbol{h} = \mathrm{diag}(h_1, h_2)$ is a deterministic diagonal matrix function with $h_j \geq 0$. We assume that $g_j, h_j, j = 1, 2$ have compact supports contained in the rectangular domain $D \subset \mathbb{R}^2$. $W(x) = (W_1(x), W_2(x))^\top$ is a two-dimensional two-parameter Brownian sheet where $W_1(x)$ and $W_2(x)$ are two independent one-dimensional two-parameter Brownian sheets . $\dot{W}_x$ is a white noise which can be thought as the derivative of the Brownian sheet W_x. To make the paper self-contained, some preliminaries are presented in the appendix for the Brownian sheet, white noise, and corresponding stochastic integrals.

In this random source model, $\boldsymbol{g}$ and $\boldsymbol{h}$ can be viewed as the mean and standard deviation of $\boldsymbol{f}$, respectively. Hence $\boldsymbol{h}^2 = \mathrm{diag}(h_1^2, h_2^2)$ is the variance of $\boldsymbol{f}$. To ensure the uniqueness of the solution, the following Kupradze-Sommerfeld radiation condition is required for the radiated wave field:

$$\lim_{r\to\infty} r^{1/2}(\partial_r \boldsymbol{u}_\mathrm{p} - \mathrm{i}\kappa_\mathrm{p}\boldsymbol{u}_\mathrm{p}) = 0, \quad \lim_{r\to\infty} r^{1/2}(\partial_r \boldsymbol{u}_\mathrm{s} - \mathrm{i}\kappa_\mathrm{s}\boldsymbol{u}_\mathrm{s}) = 0, \quad r = |x|, \tag{2.3}$$

uniformly in all directions $\hat{x} = x/|x|$, where

$$\boldsymbol{u}_\mathrm{p} = -\frac{1}{\kappa_\mathrm{p}^2}\nabla\nabla\cdot\boldsymbol{u}, \quad \boldsymbol{u}_\mathrm{s} = \frac{1}{\kappa_\mathrm{s}^2}\nabla\times(\nabla\times\boldsymbol{u})$$

are the compressional component and the shear component of $\boldsymbol{u}$, respectively, and

$$\kappa_\mathrm{p} = \frac{\omega}{\sqrt{\lambda+2\mu}}, \quad \kappa_\mathrm{s} = \frac{\omega}{\sqrt{\mu}}$$

are known as the compressional wavenumber and the shear wavenumber, respectively.

Let $B_R = \{x \in \mathbb{R}^d : |x| < R\}$ be the ball with radius R. Denote by ∂B_R the boundary of B_R. Let R be large enough such that $\bar{D} \subset B_R$. Given the random electric current density function $\boldsymbol{f}$, i.e., given $\boldsymbol{g}$ and $\boldsymbol{h}$, the direct problem is to determine the random wave field $\boldsymbol{u}$ of the stochastic scattering problem (2.1) and (2.3). The inverse problem is to determine the mean $\boldsymbol{g}$ and the standard deviation $\boldsymbol{h}$ or the variance $\boldsymbol{h}^2$ of the random source function from the measured random wave field on ∂B_R at a finite number of frequencies $\omega_k, k = 1, \ldots, K$.

2.2. Deterministic direct problem. We begin with the solution for the deterministic direct source problem. Let $\boldsymbol{h} = 0$ in (2.2), i.e., no randomness is present in the source. The stochastic scattering problem reduces to the deterministic scattering problem:

$$\begin{cases} \mu\Delta\boldsymbol{u} + (\lambda+\mu)\nabla\nabla\cdot\boldsymbol{u} + \omega^2\boldsymbol{u} = \boldsymbol{g} & \text{in } \mathbb{R}^2, \\ \partial_r\boldsymbol{u}_\mathrm{p} - \mathrm{i}\kappa_\mathrm{p}\boldsymbol{u}_\mathrm{p} = o(r^{-1/2}) & \text{as } r\to\infty, \\ \partial_r\boldsymbol{u}_\mathrm{s} - \mathrm{i}\kappa_\mathrm{s}\boldsymbol{u}_\mathrm{s} = o(r^{-1/2}) & \text{as } r\to\infty. \end{cases} \tag{2.4}$$

Given $\boldsymbol{g} \in L^2(D)^2$, it is known that the scattering problem (2.4) has a unique solution

$$\boldsymbol{u}(x,\omega) = \int_D \mathbb{G}(x,y,\omega)\boldsymbol{g}(y)\mathrm{d}y, \tag{2.5}$$

where $\mathbb{G}$ is the Green tensor function of the Navier equation:

$$\mathbb{G}(x,y,\omega)=\frac{\mathrm{i}}{4\mu}H_0^{(1)}(\kappa_{\mathrm{s}}|x-y|)\mathbb{I}+\frac{\mathrm{i}}{4\omega^2}\nabla_x\nabla_x^\top\Big[H_0^{(1)}(\kappa_{\mathrm{s}}|x-y|)-H_0^{(1)}(\kappa_{\mathrm{p}}|x-y|)\Big].$$

Here $\mathbb{I}$ is the 2×2 identity matrix, $H_0^{(1)}$ is the Hankel function of the first kind with order zero, and

$$\nabla_x\nabla_x^\top=\begin{pmatrix}\partial_{x_1x_1} & \partial_{x_1x_2}\\ \partial_{x_1x_2} & \partial_{x_2x_2}\end{pmatrix}.$$

It is known that this Green tensor function has an equivalent form

$$\mathbb{G}(x,y,\omega)=G_1(|x-y|)\mathbb{I}+G_2(|x-y|)\mathbb{J}(x-y), \tag{2.6}$$

which plays an vital role in derivation of the subsequent regularity analysis. Here for $x\in\mathbb{R}^2\backslash\{0\}$, the matrix $\mathbb{J}$ is given by

$$\mathbb{J}(x)=\frac{xx^\top}{|x|^2}.$$

It is shown in [25] that the functions G_1 and G_2 can be decomposed into

$$G_j(v)=\frac{1}{\pi}\log(v)\Phi_j(v)+\eta_j(v),\quad j=1,2, \tag{2.7}$$

where Φ_j and η_j are analytic functions. Explicitly, we have

$$\Phi_1(v)=\alpha+\beta_1v^2+O(v^4),\quad \Phi_2=\beta_2v^2+O(v^4) \tag{2.8}$$

and

$$\eta_1(v)=\gamma_1+O(v^2),\quad \eta_2=\gamma_2+O(v^2) \tag{2.9}$$

for $v\to 0$, where α, β_j, and γ_j are constants depending on ω, μ, and λ.

The following regularity results of the Green tensor function play an important role in the analysis of the stochastic direct scattering problem.

LEMMA 2.1. *Let $\Omega\subset\mathbb{R}^2$ be a bounded domain. Then $\|\mathbb{G}(\cdot,y)\|\in L^2(\Omega)$, $\forall\, y\in\Omega$, i.e.*

$$\int_\Omega\|\mathbb{G}(x,y,\omega)\|^2\mathrm{d}x<\infty,$$

where $\|\cdot\|$ is the Frobenius norm.

Proof. Let $a=\sup_{x,y\in\Omega}|x-y|$. We have $\bar{\Omega}\subset B_a(y)$, where $B_a(y)$ is the ball with radius a and center at y. Since $\|J(w)\|=1$, it follows from the expression in (2.6) and (2.7) that we only need to show that

$$\log(|x-y|)|x-y|^m\in L^2(\Omega),\quad \forall\, y\in\Omega,\ m\geq 0.$$

A simple calculation yields

$$\begin{aligned}\int_\Omega\Big|\log(|x-y|)|x-y|^m\Big|^2\mathrm{d}x&\leq\int_{B_a(y)}\Big|\log(|x-y|)|x-y|^m\Big|^2\mathrm{d}x\\ &\lesssim\int_0^a r^{1+2m}\Big|\log(r)\Big|^2\mathrm{d}r<\infty,\end{aligned}$$

which completes the proof. □

Throughout the paper, $a \lesssim b$ stands for $a \leq Cb$, where C is a positive constant and its specific value is not required but should be clear from the context.

LEMMA 2.2. *Let $\Omega \subset \mathbb{R}^2$ be a bounded domain. We have for $\alpha \in (\frac{3}{2}, \infty)$ that*

$$\int_\Omega \|\mathbb{G}(x,y,\omega) - \mathbb{G}(x,z,\omega)\|^\alpha \mathrm{d}x \lesssim |y-z|^{\frac{3}{2}}, \quad \forall\ y,z \in \Omega. \tag{2.10}$$

Proof. It follows from (2.6) and the triangle inequality that

$$\begin{aligned}
&\int_\Omega \|\mathbb{G}(x,y,\omega) - \mathbb{G}(x,z,\omega)\|^\alpha \mathrm{d}x \\
&\lesssim \int_\Omega \Big\| G_1(|x-y|)\mathbb{I} - G_1(|x-z|)\mathbb{I} \Big\|^\alpha \mathrm{d}x \\
&\qquad\qquad + \int_\Omega \Big\| G_2(|x-y|)\mathbb{J}(x-y) - G_2(|x-z|)\mathbb{J}(x-z) \Big\|^\alpha \mathrm{d}x \\
&\lesssim \int_\Omega \Big| G_1(|x-y|) - G_1(|x-z|) \Big|^\alpha \mathrm{d}x + \int_\Omega \Big| G_2(|x-y|) - G_2(|x-z|) \Big|^\alpha \|\mathbb{J}(x-y)\|^\alpha \mathrm{d}x \\
&\qquad\qquad + \int_\Omega |G_2(|x-z|)|^\alpha \|\mathbb{J}(x-y) - \mathbb{J}(x-z)\|^\alpha \mathrm{d}x \\
&=: T_1 + T_2 + T_3.
\end{aligned}$$

We shall only present the estimates of T_1 and T_3 since the estimates of T_1 and T_2 are similar due to $\|\mathbb{J}(x)\| = 1$ and (2.7).

Step 1. The estimate of T_1. It suffices to estimate the singular part G_1 of T_1. It follows from (2.7), (2.8), and (2.9) that we have

$$\begin{aligned}
T_1 \lesssim& \int_\Omega \Big| \log(|x-y|) - \log(|x-z|) \Big|^\alpha \mathrm{d}x + \int_\Omega \Big| |x-y|^p - |x-z|^p \Big|^\alpha \mathrm{d}x \\
&+ \int_\Omega \Big| \log(|x-y|)|x-y|^p - \log(|x-z|)|x-z|^p \Big|^\alpha \mathrm{d}x \\
=:& T_1^1 + T_1^2 + T_1^3,
\end{aligned}$$

where $p = 2$ or 4.

For the term T_1^1, we have

$$\begin{aligned}
T_1^1 =& \int_\Omega \Big| |x-y| - |x-z| \Big|^{\frac{3}{2}} \Big| \log(|x-y|) - \log(|x-z|) \Big|^{\alpha - \frac{3}{2}} \\
&\qquad \times \left| \int_0^1 \Big(|x-y|t + |x-z|(1-t) \Big)^{-1} \mathrm{d}t \right|^{\frac{3}{2}} \mathrm{d}x \\
\leq& |y-z|^{\frac{3}{2}} \int_\Omega \Big| \log(|x-y|) - \log(|x-z|) \Big|^{\alpha - \frac{3}{2}} \left| \frac{1}{|x-y|} + \frac{1}{|x-z|} \right|^{\frac{3}{2}} \mathrm{d}x \\
\leq& |y-z|^{\frac{3}{2}} \left(\int_\Omega \Big(\frac{1}{|x-y|} + \frac{1}{|x-z|} \Big)^{\frac{9}{5}} \mathrm{d}x \right)^{\frac{5}{6}} \\
&\qquad \times \left(\int_\Omega \Big| \log(|x-y|) - \log(|x-z|) \Big|^{6\alpha - 9} \mathrm{d}x \right)^{\frac{1}{6}},
\end{aligned}$$

where we have used the Hölder inequality in the last step.

Let $a = \sup_{x,y\in\Omega}|x-y|$ and $b = \sup_{x,z\in\Omega}|x-z|$. We have $\bar{\Omega} \subset B_a(y)$ and $\bar{\Omega} \subset B_b(z)$, where $B_a(y)$ and $B_b(z)$ are the discs with radii a and b and centers at y and z, respectively. It is easy to verify that

$$\begin{aligned}\int_\Omega \Big(\frac{1}{|x-y|}+\frac{1}{|x-z|}\Big)^{\frac{9}{5}}\mathrm{d}x &\lesssim \int_{B_a(y)}\frac{1}{|x-y|^{\frac{9}{5}}}\mathrm{d}x+\int_{B_b(z)}\frac{1}{|x-z|^{\frac{9}{5}}}\mathrm{d}x\\ &\lesssim \int_0^a r^{-\frac{4}{5}}\mathrm{d}r+\int_0^b r^{-\frac{4}{5}}\mathrm{d}r<\infty\end{aligned}$$

and

$$\begin{aligned}&\int_\Omega \Big|\log(|x-y|)-\log(|x-z|)\Big|^{6\alpha-9}\mathrm{d}x\\ &\lesssim \int_{B_a(y)}\Big|\log(|x-y|)\Big|^{6\alpha-9}\mathrm{d}x+\int_{B_b(z)}\Big|\log(|x-z|)\Big|^{6\alpha-9}\mathrm{d}x\\ &\lesssim \int_0^a r\Big|\log(r)\Big|^{6\alpha-9}\mathrm{d}r+\int_0^b r\Big|\log(r)\Big|^{6\alpha-9}\mathrm{d}r<\infty.\end{aligned}$$

Combining the above estimates gives $T_1^1 \lesssim |y-z|^{\frac{3}{2}}$.

For the term T_1^2, using the identity

$$a^p-b^p=(a-b)\big(a^{p-1}+a^{p-2}b+\cdots+ab^{p-2}+b^{p-1}\big),$$

we obtain

$$\begin{aligned}T_1^2 &\lesssim |y-z|^\alpha\int_\Omega\Big[|x-y|^{(p-1)\alpha}+|x-y|^{(p-2)\alpha}|x-z|^\alpha+\cdots+|x-z|^{(p-1)\alpha}\Big]\mathrm{d}x\\ &\lesssim |y-z|^\alpha.\end{aligned}$$

Applying the technique of estimating the terms T_1^1 and T_1^2, we get the estimate for the term T_1^3:

$$\begin{aligned}T_1^3 &\lesssim \int_\Omega\Big|\log(|x-y|)\Big|^\alpha\Big||x-y|^p-|x-z|^p\Big|^\alpha\mathrm{d}x\\ &\qquad+\int_\Omega\Big|\log(|x-y|)-\log(|x-z|)\Big|^\alpha|x-z|^{p\alpha}\mathrm{d}x\\ &\lesssim |y-z|^\alpha\int_\Omega\Big|\log(|x-y|)\Big|^\alpha\Big[|x-y|^{(p-1)\alpha}+|x-y|^{(p-2)\alpha}|x-z|^\alpha+\cdots+|x-z|^{(p-1)\alpha}\Big]\mathrm{d}x\\ &\quad+|y-z|^{\frac{3}{2}}\int_\Omega\Big|\log(|x-y|)-\log(|x-z|)\Big|^{\alpha-\frac{3}{2}}\left|\frac{1}{|x-y|}+\frac{1}{|x-z|}\right|^{\frac{3}{2}}|x-z|^{p\alpha}\mathrm{d}x\\ &\lesssim |y-z|^\alpha+|y-z|^{\frac{3}{2}}.\end{aligned}$$

Therefore, we obtain $T_1 \le |y-z|^{\frac{3}{2}}$ for $\alpha > \frac{3}{2}$. Similarly, we may have the estimate $T_2 \le |y-z|^{\frac{3}{2}}$.

Step 2. The estimate of term T_3. Recall

$$\mathbb{J}(x)=\begin{bmatrix}J_{11}(x) & J_{12}(x)\\ J_{12}(x) & J_{22}(x)\end{bmatrix}=\begin{bmatrix}\frac{x_1^2}{|x|^2} & \frac{x_1x_2}{|x|^2}\\ \frac{x_1x_2}{|x|^2} & \frac{x_2^2}{|x|^2}\end{bmatrix}.$$

A simple calculation yields

$$\begin{aligned}\|\mathbb{J}(x-y)-\mathbb{J}(x-z)\|^2 &= |J_{11}(x-y)-J_{11}(x-z)|^2\\ &\quad + 2|J_{12}(x-y)-J_{12}(x-z)|^2 + |J_{22}(x-y)-J_{22}(x-z)|^2.\end{aligned}$$

It is easy to verify that

$$\begin{aligned}&|J_{11}(x-y)-J_{11}(x-z)|\\ =&\left|\frac{(x_1-y_1)^2}{|x-y|^2}-\frac{(x_1-z_1)^2}{|x-z|^2}\right|\\ =&\left|\Big(\frac{x_1-y_1}{|x-y|}+\frac{x_1-z_1}{|x-z|}\Big)\Big(\frac{x_1-y_1}{|x-y|}-\frac{x_1-z_1}{|x-z|}\Big)\right|\\ \lesssim&\left|\frac{x_1-y_1}{|x-y|}-\frac{x_1-z_1}{|x-z|}\right|\\ =&\left|\frac{\big(|x-z|-|x-y|\big)(x_1-y_1)+|x-y|\big((x_1-y_1)-(x_1-z_1)\big)}{|x-y||x-z|}\right|\\ \lesssim&\frac{|y-z|}{|x-z|}.\end{aligned}$$

Similarly, we may show that

$$|J_{22}(x-y)-J_{22}(x-z)| = \left|\frac{(x_2-y_2)^2}{|x-y|^2}-\frac{(x_2-z_2)^2}{|x-z|^2}\right| \lesssim \frac{|y-z|}{|x-z|}$$

and

$$\begin{aligned}|J_{12}(x-y)-J_{12}(x-z)| =& \left|\frac{(x_1-y_1)(x_2-y_2)}{|x-y|^2}-\frac{(x_1-z_1)(x_2-z_2)}{|x-z|^2}\right|\\ \le& \left|\frac{(x_1-y_1)(x_2-y_2)}{|x-y|^2}-\frac{(x_1-y_1)(x_2-y_2)}{|x-z|^2}\right|\\ &+\left|\frac{(x_1-y_1)(x_2-y_2)}{|x-z|^2}-\frac{(x_1-z_1)(x_2-z_2)}{|x-z|^2}\right|\\ \le&\frac{|y-z|}{|x-z|}+\frac{|x-y|}{|x-z|^2}|y-z|.\end{aligned}$$

Hence

$$\|\mathbb{J}(x-y)-\mathbb{J}(x-z)\| \lesssim \frac{|y-z|}{|x-z|}+\frac{|x-y|}{|x-z|^2}|y-z|$$

and

$$\|\mathbb{J}(x-y)-\mathbb{J}(x-z)\| \lesssim \frac{|y-z|}{|x-y|}+\frac{|x-z|}{|x-y|^2}|y-z|.$$

Again, it suffices to consider the singular part G_2 of T_3. Using (2.7), (2.8), and (2.9), we split the term T_3 into two parts:

$$\begin{aligned}T_3 \lesssim& \int_\Omega \Big|\log(|x-z|)\Big[|x-z|^2+|x-z|^4\Big]+|x-z|^2\Big|^\alpha \|\mathbb{J}(x-y)-\mathbb{J}(x-z)\|^\alpha \mathrm{d}x\\ &+\int_\Omega \|\mathbb{J}(x-y)-\mathbb{J}(x-z)\|^\alpha \mathrm{d}x\\ =:&T_3^1+T_3^2.\end{aligned}$$

For the term T_3^1, we have

$$\begin{aligned} T_3^1 \lesssim & |y-z|^\alpha \int_\Omega \Big| \log(|x-z|) \Big[|x-z|^2 + |x-z|^4 \Big] + |x-z|^2 \Big|^\alpha \Big[\frac{1}{|x-z|^\alpha} + \frac{|x-y|^\alpha}{|x-z|^{2\alpha}} \Big] \mathrm{d}x \\ \lesssim & |y-z|^\alpha. \end{aligned}$$

The estimate of T_3^2 is more technical. We let $\xi = \frac{y+z}{2}$ and $r = |y-z|$. It is clear to note that

$$\begin{aligned} T_3^2 = & \left(\int_{B_{\frac{r}{4}}(y)} + \int_{B_{\frac{r}{4}}(z)} + \int_{B_{2r}(\xi) \backslash B_{\frac{r}{4}}(y) \cup B_{\frac{r}{4}}(z)} + \int_{\Omega \backslash B_{2r}(\xi)} \right) \| \mathbb{J}(x-y) - \mathbb{J}(x-z) \|^\alpha \mathrm{d}x \\ =: & \, I_1 + I_2 + I_3 + I_4. \end{aligned}$$

Next we estimate the above four parts. First we have

$$I_1 \lesssim \int_{B_{\frac{r}{4}}(y)} \frac{r^\alpha}{|x-z|^\alpha} + \frac{|x-y|^\alpha}{|x-z|^{2\alpha}} r^\alpha \mathrm{d}x \lesssim \int_{B_{\frac{r}{4}}(y)} \mathrm{d}x \lesssim r^2,$$

where we have utilized the fact that $|x-y| \leq \frac{r}{4}$ and $|x-z| > \frac{r}{2}$ for $x \in B_{\frac{r}{4}}(y)$. Similarly, we have

$$I_2 \lesssim \int_{B_{\frac{r}{4}}(z)} \frac{r^\alpha}{|x-y|^\alpha} + \frac{|x-z|^\alpha}{|x-y|^{2\alpha}} r^\alpha \mathrm{d}x \lesssim r^2.$$

For the term I_3, we have $|x-z| \geq \frac{r}{4}$ and $\frac{r}{4} \leq |x-y| < 3r$ for any $x \in B_{2r}(\xi) \backslash B_{\frac{r}{4}}(y) \cup B_{\frac{r}{4}}(z)$. Thus

$$I_3 \leq \int_{B_{2r}(\xi) \backslash B_{\frac{r}{4}}(y) \cup B_{\frac{r}{4}}(z)} \frac{r^\alpha}{|x-z|^\alpha} + \frac{|x-y|^\alpha}{|x-z|^{2\alpha}} r^\alpha \mathrm{d}x \lesssim \int_{B_{2r}(\xi) \backslash B_{\frac{r}{4}}(y) \cup B_{\frac{r}{4}}(z)} \mathrm{d}x \lesssim r^2.$$

It is clear to note for $x \in \Omega \backslash B_{2r}(\xi)$ that

$$\left| \frac{|x-\xi|}{|x-y|} - 1 \right| \leq \frac{|\xi - y|}{|x-y|} \leq \frac{r/2}{2r - r/2} = \frac{1}{3}.$$

We have

$$\frac{2}{3}|x-y| \leq |x-\xi| \leq \frac{4}{3}|x-y|$$

and

$$\frac{2}{3}|x-z| \leq |x-\xi| \leq \frac{4}{3}|x-z|,$$

which give

$$\begin{aligned} I_4 \lesssim & \int_{\Omega \backslash B_{2r}(\xi)} \frac{r^\alpha}{|x-z|^\alpha} + \frac{|x-y|^\alpha}{|x-z|^{2\alpha}} r^\alpha \mathrm{d}x \\ \lesssim & \int_{\Omega \backslash B_{2r}(\xi)} \frac{r^\alpha}{|x-\xi|^\alpha} \mathrm{d}x \\ \lesssim & \, r^\alpha \int_{2r}^R s^{1-\alpha} ds \lesssim r^\alpha \Big[R^{2-\alpha} + (2r)^{2-\alpha} \Big] \lesssim r^\alpha + r^2, \end{aligned}$$

where $\bar{\Omega} \subset B_R(\xi)$ with $B_R(\xi)$ being the disc with radius R and center at ξ. Combining all the estimates in step 2 gives $T_3 \lesssim |y-z|^{\min\{\alpha, 2\}}$.

The proof is completed by combining step 1 and step 2. □

2.3. Stochastic direct problem. In this section, we discuss the solution for the stochastic direct source scattering problem:

$$\begin{cases} \mu\Delta \boldsymbol{u} + (\lambda+\mu)\nabla\nabla\cdot\boldsymbol{u} + \omega^2\boldsymbol{u} = \boldsymbol{g} + \boldsymbol{h}\dot{W}_x & \text{in } \mathbb{R}^2, \\ \partial_r \boldsymbol{u}_{\rm p} - {\rm i}\kappa_{\rm p}\boldsymbol{u}_{\rm p} = o(r^{-1/2}) & \text{as } r\to\infty, \\ \partial_r \boldsymbol{u}_{\rm s} - {\rm i}\kappa_{\rm s}\boldsymbol{u}_{\rm s} = o(r^{-1/2}) & \text{as } r\to\infty. \end{cases} \tag{2.11}$$

Let us first specify the regularity of $\boldsymbol{g}$ and $\boldsymbol{h}$ before discussing the solution of the stochastic scattering problem (2.11). Motivated by the solution of the deterministic direct problem (2.4), we assume that $\boldsymbol{g} \in L^2(D)^2$. The regularity of $\boldsymbol{h}$ is chosen such that the stochastic integral

$$\int_D \mathbb{G}(x,y,\omega)\boldsymbol{h}(y){\rm d}W_y$$

satisfies

$$\begin{aligned} \mathbf{E}\Big(\Big|\int_D \mathbb{G}(x,y,\omega)\boldsymbol{h}(y){\rm d}W_y\Big|^2\Big) &= \int_D \|\mathbb{G}(x,y,\omega)\boldsymbol{h}(y)\|^2{\rm d}y \\ &\le \int_D \|\mathbb{G}(x,y,\omega)\|^2\|\boldsymbol{h}(y)\|^2{\rm d}x < \infty, \end{aligned}$$

where Proposition A.2 is used in the above identity.

We only need to consider the singular part of the Green tensor function. It follows from the Hölder inequality that

$$\int_D \Big|\log(|x-y|)|x-y|^m\Big|^2\|\boldsymbol{h}(y)\|^2{\rm d}y \le \Big(\int_D \Big|\log(|x-y|)|x-y|^m\Big|^{\frac{2p}{p-2}}{\rm d}y\Big)^{\frac{p-2}{p}} \Big(\int_D \|\boldsymbol{h}(y)\|^p{\rm d}y\Big)^{\frac{2}{p}}.$$

Since the first term on the right-hand side of the above inequality is a singular integral, p should be chosen such that it is well defined. Let $\rho > 0$ be sufficiently large such that $\bar{D} \subset B_\rho(x)$, where $B_\rho(x)$ is the disc with radius ρ and center at x. A simple calculation yields

$$\begin{aligned} \int_D \Big|\log(|x-y|)|x-y|^m\Big|^{\frac{2p}{p-2}}{\rm d}y &\le \int_{B_\rho(x)} \Big|\log(|x-y|)|x-y|^m\Big|^{\frac{2p}{p-2}}{\rm d}y \\ &\lesssim \int_0^\rho r^{1+\frac{2mp}{p-2}}\Big|\log(r)\Big|^{\frac{2p}{p-2}}{\rm d}r. \end{aligned}$$

It is clear to note that the above integral is well defined when $p > 2$.

From now on, we assume that $h_j \in L^p(D), j = 1, 2$ where $p \in (2, \infty]$. Moreover, we require that $h_j \in C^{0,\eta}(D)$, i.e., η-Hölder continuous, where $\eta \in (0, 1]$. The Hölder continuity will be used in the analysis for existence of the solution.

The following theorem shows the well-posedness of the solution for the stochastic scattering problem (2.11). The explicit solution will be used to derive Fredholm integral equations for the inverse problem.

THEOREM 2.3. *Let $\Omega \subset \mathbb{R}^2$ be a bounded domain. There exists a unique continuous stochastic process $\boldsymbol{u} : \Omega \to \mathbb{C}$ satisfying*

$$\boldsymbol{u}(x,\omega) = \int_D \mathbb{G}(x,y,\omega)\boldsymbol{g}(y){\rm d}y + \int_D \mathbb{G}(x,y,\omega)\boldsymbol{h}(y){\rm d}W_y, \quad a.s., \tag{2.12}$$

which is called the mild solution of the stochastic scattering problem (2.11).

Proof. First we show that there exists a continuous modification of the random field

$$\boldsymbol{v}(x,\omega) = \int_D \mathbb{G}(x,y,\omega)\boldsymbol{h}(y)\mathrm{d}W_y, \quad x \in \Omega.$$

For any $x, z \in \Omega$, we have from Proposition A.2 and the Hölder inequality that

$$\begin{aligned}\mathbf{E}(|\boldsymbol{v}(x,\omega)-\boldsymbol{v}(z,\omega)|^2) &= \int_D \Big\| \Big(\mathbb{G}(x,y,\omega)-\mathbb{G}(z,y,\omega)\Big)\boldsymbol{h}(y)\Big\|^2 \mathrm{d}y \\ &\le \left(\int_D \|\mathbb{G}(x,y,\omega)-\mathbb{G}(z,y,\omega)\|^{\frac{2p}{p-2}}\mathrm{d}y\right)^{\frac{p-2}{p}} \left(\int_D \|\boldsymbol{h}(y)\|^p \mathrm{d}y\right)^{\frac{2}{p}}.\end{aligned}$$

For $p > 2$, it follows from (2.10) that

$$\int_D \|\mathbb{G}(x,y,\omega)-\mathbb{G}(z,y,\omega)\|^{\frac{2p}{p-2}}\mathrm{d}y \lesssim |x-z|^{\frac{3}{2}},$$

which gives

$$\mathbf{E}(|\boldsymbol{v}(x,\omega)-\boldsymbol{v}(z,\omega)|^2) \lesssim \|\boldsymbol{h}\|^2_{L^p(D)^2}|x-z|^{\frac{3p-6}{2p}}.$$

Since $\boldsymbol{v}(x,\kappa)-\boldsymbol{v}(z,\kappa)$ is a random Gaussian variable, we have (cf. [22, Proposition 3.14]) for any integer q that

$$\mathbf{E}(|\boldsymbol{v}(x,\omega)-\boldsymbol{v}(z,\omega)|^{2q}) \lesssim \big(\mathbf{E}(|\boldsymbol{v}(x,\omega)-\boldsymbol{v}(z,\omega)|^2)\big)^q \lesssim \|\boldsymbol{h}\|^{2q}_{L^p(D)^2}|x-z|^{\frac{q(3p-6)}{2p}}.$$

Taking $q > \frac{2p}{3p-6}$, we obtain from Kolmogorov's continuity theorem that there exists a P-a.s. continuous modification of the random field $\boldsymbol{v}$.

Clearly, the uniqueness of the mild solution comes from the solution representation formula (2.12), which depends only on the Green function $\mathbb{G}$ and the source functions $\boldsymbol{g}$ and $\boldsymbol{h}$.

Next we present a constructive proof to show the existence. We construct a sequence of processes $\dot{W}^n_x$ satisfying $\boldsymbol{h}\dot{W}^n \in L^2(D)^2$ and a sequence

$$\boldsymbol{v}^n(x,\omega) = \int_D \mathbb{G}(x,y,\omega)\boldsymbol{h}(y)\mathrm{d}W^n_y, \quad x \in \Omega,$$

which satisfies $\boldsymbol{v}^n \to \boldsymbol{v}$ in $L^2(\Omega)$ a.s. as $n \to \infty$.

Let $\mathcal{T}_n = \cup_{j=1}^n K_j$ be a regular triangulation of D, where K_j are triangles. Denote

$$\xi_j = |K_j|^{-\frac{1}{2}} \int_{K_j} \mathrm{d}W_x, \quad 1 \le j \le n,$$

where $|K_j|$ is the area of the K_j. It is known in [12] that ξ_j is a family of independent identically distributed normal random variables with mean zero and variance one. The piecewise constant approximation sequence is given by

$$\dot{W}^n_x = \sum_{j=1}^n |K_j|^{-\frac{1}{2}}\xi_j\chi_j(x),$$

where χ_j is the characteristic function of K_j. Clearly we have for any $p \geq 1$ that

$$\begin{aligned}\mathbf{E}\big(\|\dot{W}^n\|^p_{L^p(D)^2}\big) &= \mathbf{E}\Big(\int_D \Big|\sum_{j=1}^n |K_j|^{-\frac{1}{2}}\xi_j\chi_j(x)\Big|^p \mathrm{d}x\Big) \lesssim \mathbf{E}\Big(\int_D \sum_{j=1}^n |K_j|^{-\frac{p}{2}}|\xi_j|^p\chi_j(x)\mathrm{d}x\Big)\\ &= \sum_{j=1}^n \mathbf{E}(|\xi_j|^p)|K_j|^{1-\frac{p}{2}} < \infty,\end{aligned}$$

which shows that $\dot{W}^n \in L^p(D)^2, p \geq 1$. It follows from the Hölder inequality that $\boldsymbol{h}\dot{W}^n \in L^2(D)^2$.

Using Proposition A.2, we have that

$$\begin{aligned}&\mathbf{E}\Big(\int_\Omega \Big|\int_D \mathbb{G}(x,y,\omega)\boldsymbol{h}(y)\mathrm{d}W_y - \int_D \mathbb{G}(x,y,\omega)\boldsymbol{h}(y)\mathrm{d}W_y^n\Big|^2\mathrm{d}x\Big)\\
&= \mathbf{E}\Big(\int_\Omega \Big|\sum_{j=1}^n \int_{K_j} \mathbb{G}(x,y,\omega)\boldsymbol{h}(y)\mathrm{d}W_y - \sum_{j=1}^n |K_j|^{-1}\int_{K_j}\mathbb{G}(x,z,\omega)\boldsymbol{h}(z)\mathrm{d}z\int_{K_j}\mathrm{d}W_y\Big|^2\mathrm{d}x\Big)\\
&= \mathbf{E}\Big(\int_\Omega \Big|\sum_{j=1}^n \int_{K_j}\int_{K_j} |K_j|^{-1}(\mathbb{G}(x,y,\omega)\boldsymbol{h}(y) - \mathbb{G}(x,z,\omega)\boldsymbol{h}(z))\mathrm{d}z\mathrm{d}W_y\Big|^2\mathrm{d}x\Big)\\
&= \int_\Omega \Big(\sum_{j=1}^n \int_{K_j}\Big||K_j|^{-1}\int_{K_j}(\mathbb{G}(x,y,\omega)\boldsymbol{h}(y) - \mathbb{G}(x,z,\omega)\boldsymbol{h}(z))\mathrm{d}z\Big|^2\mathrm{d}y\Big)\mathrm{d}x\\
&\leq \int_\Omega \Big(\sum_{j=1}^n |K_j|^{-1}\int_{K_j}\int_{K_j}\|\mathbb{G}(x,y,\omega)\boldsymbol{h}(y) - \mathbb{G}(x,z,\omega)\boldsymbol{h}(z)\|^2\mathrm{d}z\mathrm{d}y\Big)\mathrm{d}x\\
&= \sum_{j=1}^n |K_j|^{-1}\int_{K_j}\int_{K_j}\int_\Omega \|\mathbb{G}(x,y,\omega)\boldsymbol{h}(y) - \mathbb{G}(x,z,\omega)\boldsymbol{h}(z)\|^2\mathrm{d}x\mathrm{d}z\mathrm{d}y.\end{aligned}$$

Using the triangle and Cauchy-Schwartz inequalities, we get

$$\begin{aligned}\int_\Omega \|\mathbb{G}(x,y,\omega)\boldsymbol{h}(y) - \mathbb{G}(x,z,\omega)\boldsymbol{h}(z)\|^2\mathrm{d}x &\lesssim \int_\Omega \|\mathbb{G}(x,y,\omega) - \mathbb{G}(x,z,\omega)\|^2\|\boldsymbol{h}(y)\|^2\mathrm{d}x\\ &\quad + \int_\Omega \|\mathbb{G}(x,z,\omega)\|^2\|\boldsymbol{h}(y) - \boldsymbol{h}(z)\|^2\mathrm{d}x.\end{aligned}$$

It follows from (2.10), Lemma 2.1, and the η-Hölder continuity of $\boldsymbol{h}$ that

$$\int_\Omega \|\mathbb{G}(x,y,\omega)\boldsymbol{h}(y) - \mathbb{G}(x,z,\omega)\boldsymbol{h}(z)\|^2\mathrm{d}x \lesssim \|\boldsymbol{h}(y)\|^2|y-z|^{\frac{3}{2}} + |y-z|^{2\eta},$$

which gives

$$\begin{aligned}&\mathbf{E}\Big(\int_\Omega \Big|\int_D \mathbb{G}(x,y,\omega)\boldsymbol{h}(y)\mathrm{d}W_y - \int_D \mathbb{G}(x,y,\omega)\boldsymbol{h}(y)\mathrm{d}W_y^n\Big|^2\mathrm{d}x\Big)\\
&\lesssim \sum_{j=1}^n |K_j|^{-1}\int_{K_j}\int_{K_j}\|\boldsymbol{h}(z)\|^2|y-z|^{\frac{3}{2}}\mathrm{d}z\mathrm{d}y + \sum_{j=1}^n |K_j|^{-1}\int_{K_j}\int_{K_j}|y-z|^{2\eta}\mathrm{d}z\mathrm{d}y\\
&\leq \|\boldsymbol{h}\|^2_{L^2(D)^2}\max_{1\leq j\leq n}(\mathrm{diam}K_j)^{\frac{3}{2}} + |D|\max_{1\leq j\leq n}(\mathrm{diam}K_j)^{2\eta} \to 0\end{aligned}$$

as $n \to \infty$ since the diameter of $K_j \to 0$ as $n \to \infty$.

For each $n \in \mathbb{N}$, we consider the scattering problem:

$$\begin{cases} \mu\Delta \boldsymbol{u}^n + (\lambda+\mu)\nabla\nabla\cdot \boldsymbol{u}^n + \omega^2 \boldsymbol{u}^n = \boldsymbol{g} + \boldsymbol{h}\dot{W}_x^n & \text{in } \mathbb{R}^2, \\ \partial_r \boldsymbol{u}_{\mathrm{p}}^n - \mathrm{i}\kappa_{\mathrm{p}} \boldsymbol{u}_{\mathrm{p}}^n = o(r^{-1/2}) & \text{as } r \to \infty, \\ \partial_r \boldsymbol{u}_{\mathrm{s}}^n - \mathrm{i}\kappa_{\mathrm{s}} \boldsymbol{u}_{\mathrm{s}}^n = o(r^{-1/2}) & \text{as } r \to \infty. \end{cases} \tag{2.13}$$

It follows from $\boldsymbol{h}\dot{W}_x^n \in L^2(D)^2$ that the problem (2.13) has a unique solution which is given by

$$\boldsymbol{u}^n(x,\omega) = \int_D \mathbb{G}(x,y,\omega)\boldsymbol{g}(y)\mathrm{d}y + \int_D \mathbb{G}(x,y,\omega)\boldsymbol{h}(y)\mathrm{d}W_y^n. \tag{2.14}$$

Since $\mathbf{E}(\|\boldsymbol{v}^n - \boldsymbol{v}\|^2_{L^2(\Omega)^2}) \to 0$ as $n \to \infty$, there exists a subsequence still denoted as $\{\boldsymbol{v}^n\}$ which converges to $\boldsymbol{v}$ a.s.. Letting $n \to \infty$ in (2.14), we obtain the mild solution (2.12) and complete the proof. □

It is clear to note that the mild solution of the stochastic direct problem (2.12) reduces to the solution of the deterministic direct problem (2.5) when $\boldsymbol{h} = 0$, i.e., no randomness is present in the source.

3. Stochastic inverse problem. In this section, we derive the Fredholm integral equations and present a regularized Kaczmarz method to solve the stochastic inverse problem by using multiple frequency data.

3.1. Integral equations. Recall the mild solution of the stochastic direct scattering problem at angular frequency ω_k:

$$\boldsymbol{u}(x,\omega_k) = \int_D \mathbb{G}(x,y,\omega_k)\boldsymbol{g}(y)\mathrm{d}y + \int_D \mathbb{G}(x,y,\omega_k)\boldsymbol{h}(y)\mathrm{d}W_y. \tag{3.1}$$

Taking the expectation on both sides of (3.1) and using the identity

$$\mathbf{E}\Big(\int_D \mathbb{G}(x,y,\omega_k)\boldsymbol{h}(y)\mathrm{d}W_y\Big) = 0,$$

we obtain

$$\mathbf{E}(\boldsymbol{u}(x,\omega_k)) = \int_D \mathbb{G}(x,y,\omega_k)\boldsymbol{g}(y)\mathrm{d}y,$$

which is a complex-valued Fredholm integral equation of the first kind and may be used to reconstruct $\boldsymbol{g}$. However, it is more convenient to solve real-valued equations. We shall split all the complex-valued quantities into their real and imaginary parts, which also allows us to deduce the equations for the variance.

Let $\boldsymbol{u} = \mathrm{Re}\boldsymbol{u} + \mathrm{iIm}\boldsymbol{u}$ and $\mathbb{G} = \mathrm{Re}\mathbb{G} + \mathrm{iIm}\mathbb{G}$. Using (2.6), we have more explicit formulas of G_1 and G_2:

$$G_1(v) = \frac{\mathrm{i}}{4\mu}H_0^{(1)}(\kappa_{\mathrm{s}}v) - \frac{\mathrm{i}}{4\omega^2 v}\Big[\kappa_{\mathrm{s}}H_1^{(1)}(\kappa_{\mathrm{s}}v) - \kappa_{\mathrm{p}}H_1^{(1)}(\kappa_{\mathrm{p}}v)\Big]$$

and

$$G_2(v) = \frac{\mathrm{i}}{4\omega^2}\Big[\frac{2\kappa_{\mathrm{s}}}{v}H_1^{(1)}(\kappa_{\mathrm{s}}v) - \kappa_{\mathrm{s}}^2 H_0^{(1)}(\kappa_{\mathrm{s}}v) - \frac{2\kappa_{\mathrm{p}}}{v}H_1^{(1)}(\kappa_{\mathrm{p}}v) + \kappa_{\mathrm{p}}^2 H_0^{(1)}(\kappa_{\mathrm{p}}v)\Big],$$

where $H_0^{(1)}$ and $H_1^{(1)}$ are the Hankel functions of the first kind with order zero and one, respectively.

Denote

$$\kappa_{\mathrm{p},k} = \frac{\omega_k}{\sqrt{\lambda+2\mu}}, \quad \kappa_{\mathrm{s},k} = \frac{\omega_k}{\sqrt{\mu}}.$$

Let

$$\mathrm{Re}\mathbb{G}(x,y,\omega_k) = \begin{bmatrix} G_{\mathrm{Re}}^{[11]}(x,y,\omega_k) & G_{\mathrm{Re}}^{[12]}(x,y,\omega_k) \\ G_{\mathrm{Re}}^{[21]}(x,y,\omega_k) & G_{\mathrm{Re}}^{[22]}(x,y,\omega_k) \end{bmatrix},$$

where

$$\begin{aligned}
G_{\mathrm{Re}}^{[11]}(x,y,\omega_k) =& -\frac{1}{4\mu}Y_0(\kappa_{\mathrm{s},k}|x-y|) + \frac{1}{4\omega_k^2|x-y|}\Big(\kappa_{\mathrm{s},k}Y_1(\kappa_{\mathrm{s},k}|x-y|) \\
&- \kappa_{\mathrm{p},k}Y_1(\kappa_{\mathrm{p},k}|x-y|)\Big) - \frac{(x_1-y_1)^2}{4\omega_k^2|x-y|^2}\Big[\frac{2\kappa_{\mathrm{s},k}}{|x-y|}Y_1(\kappa_{\mathrm{s},k}|x-y|) \\
&- \kappa_{\mathrm{s},k}^2Y_0(\kappa_{\mathrm{s},k}|x-y|) - \frac{2\kappa_{\mathrm{p},k}}{|x-y|}Y_1(\kappa_{\mathrm{p},k}|x-y|) + \kappa_{\mathrm{p},k}^2Y_0(\kappa_{\mathrm{p},k}|x-y|)\Big], \\
G_{\mathrm{Re}}^{[12]}(x,y,\omega_k) =& -\frac{(x_1-y_1)(x_2-y_2)}{4\omega_k^2|x-y|^2}\Big[\frac{2\kappa_{\mathrm{s},k}}{|x-y|}Y_1(\kappa_{\mathrm{s},k}|x-y|) - \kappa_{\mathrm{s},k}^2Y_0(\kappa_{\mathrm{s},k}|x-y|) \\
&- \frac{2\kappa_{\mathrm{p},k}}{|x-y|}Y_1(\kappa_{\mathrm{p},k}|x-y|) + \kappa_{\mathrm{p},k}^2Y_0(\kappa_{\mathrm{p},k}|x-y|)\Big], \\
G_{\mathrm{Re}}^{[21]}(x,y,\omega_k) =& G_{\mathrm{Re}}^{[12]}(x,y,\omega_k), \\
G_{\mathrm{Re}}^{[22]}(x,y,\omega_k) =& -\frac{1}{4\mu}Y_0(\kappa_{\mathrm{s},k}|x-y|) + \frac{1}{4\omega_k^2|x-y|}\Big(\kappa_{\mathrm{s},k}Y_1(\kappa_{\mathrm{s},k}|x-y|) \\
&- \kappa_{\mathrm{p},k}Y_1(\kappa_{\mathrm{p},k}|x-y|)\Big) - \frac{(x_2-y_2)^2}{4\omega_k^2|x-y|^2}\Big[\frac{2\kappa_{\mathrm{s},k}}{|x-y|}Y_1(\kappa_{\mathrm{s},k}|x-y|) \\
&- \kappa_{\mathrm{s},k}^2Y_0(\kappa_{\mathrm{s},k}|x-y|) - \frac{2\kappa_{\mathrm{p},k}}{|x-y|}Y_1(\kappa_{\mathrm{p},k}|x-y|) + \kappa_{\mathrm{p},k}^2Y_0(\kappa_{\mathrm{p},k}|x-y|)\Big],
\end{aligned}$$

and

$$\mathrm{Im}\mathbb{G}(x,y,\omega_k) = \begin{bmatrix} G_{\mathrm{Im}}^{[11]}(x,y,\omega_k) & G_{\mathrm{Im}}^{[12]}(x,y,\omega_k) \\ G_{\mathrm{Im}}^{[21]}(x,y,\omega_k) & G_{\mathrm{Im}}^{[22]}(x,y,\omega_k) \end{bmatrix},$$

where

$$
\begin{aligned}
G_{\mathrm{Im}}^{[11]}(x,y,\omega_k) =& \frac{1}{4\mu}J_0(\kappa_{\mathrm{s},k}|x-y|) - \frac{1}{4\omega_k^2|x-y|}\Big(\kappa_{\mathrm{s},k}J_1(\kappa_{\mathrm{s},k}|x-y|) \\
&- \kappa_{\mathrm{p},k}J_1(\kappa_{\mathrm{p},k}|x-y|)\Big) + \frac{(x_1-y_1)^2}{4\omega_k^2|x-y|^2}\Big[\frac{2\kappa_{\mathrm{s},k}}{|x-y|}J_1(\kappa_{\mathrm{s},k}|x-y|) \\
&- \kappa_{\mathrm{s},k}^2J_0(\kappa_{\mathrm{s},k}|x-y|) - \frac{2\kappa_{\mathrm{p},k}}{|x-y|}J_1(\kappa_{\mathrm{p},k}|x-y|) + \kappa_{\mathrm{p},k}^2J_0(\kappa_{\mathrm{p},k}|x-y|)\Big], \\
G_{\mathrm{Im}}^{[12]}(x,y,\omega_k) =& \frac{(x_1-y_1)(x_2-y_2)}{4\omega_k^2|x-y|^2}\Big[\frac{2\kappa_{\mathrm{s},k}}{|x-y|}J_1(\kappa_{\mathrm{s},k}|x-y|) - \kappa_{\mathrm{s},k}^2J_0(\kappa_{\mathrm{s},k}|x-y|) \\
&- \frac{2\kappa_{\mathrm{p},k}}{|x-y|}J_1(\kappa_{\mathrm{p},k}|x-y|) + \kappa_{\mathrm{p},k}^2J_0(\kappa_{\mathrm{p},k}|x-y|)\Big], \\
G_{\mathrm{Im}}^{[21]}(x,y,\omega_k) =& G_{\mathrm{Im}}^{[12]}(x,y,\omega_k), \\
G_{\mathrm{Im}}^{[22]}(x,y,\omega_k) =& \frac{1}{4\mu}J_0(\kappa_{\mathrm{s},k}|x-y|) - \frac{1}{4\omega_k^2|x-y|}\Big(\kappa_{\mathrm{s},k}J_1(\kappa_{\mathrm{s},k}|x-y|) \\
&- \kappa_{\mathrm{p},k}J_1(\kappa_{\mathrm{p},k}|x-y|)\Big) + \frac{(x_2-y_2)^2}{4\omega_k^2|x-y|^2}\Big[\frac{2\kappa_{\mathrm{s},k}}{|x-y|}J_1(\kappa_{\mathrm{s},k}|x-y|) \\
&- \kappa_{\mathrm{s},k}^2J_0(\kappa_{\mathrm{s},k}|x-y|) - \frac{2\kappa_{\mathrm{p},k}}{|x-y|}J_1(\kappa_{\mathrm{p},k}|x-y|) + \kappa_{\mathrm{p},k}^2J_0(\kappa_{\mathrm{p},k}|x-y|)\Big].
\end{aligned}
$$

Here J_0, Y_0 and J_1, Y_1 are the Bessel function of the first and second kind with order zero and order 1, respectively. Clearly, the matrices $\mathrm{Re}\mathbb{G}(x,y,\omega_k)$ and $\mathrm{Im}\mathbb{G}(x,y,\omega_k)$ are symmetric.

The mild solution (3.1) can be split into the real and imaginary parts:

$$
\mathrm{Re}\boldsymbol{u}(x,\omega_k) = \int_D \mathrm{Re}\mathbb{G}(x,y,\omega_k)\boldsymbol{g}(y)\mathrm{d}y + \int_D \mathrm{Re}\mathbb{G}(x,y,\omega_k)\boldsymbol{h}(y)\mathrm{d}W_y \tag{3.2}
$$

and

$$
\mathrm{Im}\boldsymbol{u}(x,\omega_k) = \int_D \mathrm{Im}\mathbb{G}(x,y,\omega_k)\boldsymbol{g}(y)\mathrm{d}y + \int_D \mathrm{Im}\mathbb{G}(x,y,\omega_k)\mathbf{h}(y)\mathrm{d}W_y. \tag{3.3}
$$

Noting

$$
\mathbf{E}\Big(\int_D \mathrm{Re}\mathbb{G}(x,y,\omega_k)\boldsymbol{h}(y)\mathrm{d}W_y\Big) = 0 \quad \text{and} \quad \mathbf{E}\Big(\int_D \mathrm{Im}\mathbb{G}(x,y,\omega_k)\boldsymbol{h}(y)\mathrm{d}W_y\Big) = 0,
$$

we take the expectation on both sides of (3.2) and (3.3) and obtain real-valued Fredholm integral equations of the first kind to reconstruct $\boldsymbol{g}$:

$$
\begin{aligned}
\mathbf{E}(\mathrm{Re}\boldsymbol{u}(x,\omega_k)) &= \int_D \mathrm{Re}\mathbb{G}(x,y,\omega_k)\boldsymbol{g}(y)\mathrm{d}y, \\
\mathbf{E}(\mathrm{Im}\boldsymbol{u}(x,\omega_k)) &= \int_D \mathrm{Im}\mathbb{G}(x,y,\omega_k)\boldsymbol{g}(y)\mathrm{d}y,
\end{aligned}
$$

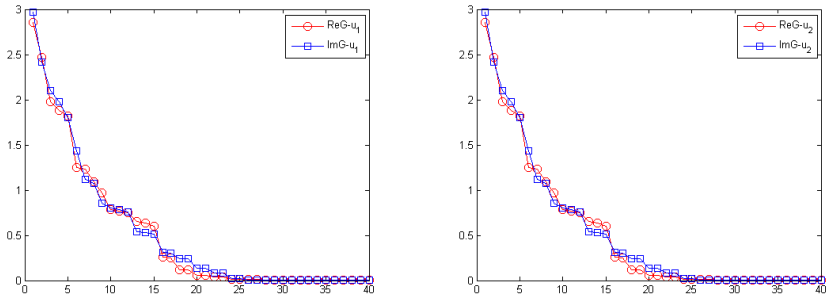

FIG. 3.1. *Singular values of the Fredholm integral equations for the reconstruction of* $\boldsymbol{g}$*: (left) component for* u_1*; (right) component for* u_2*.*

which are equivalent to the following equations in component-wise forms:

$$\mathbf{E}(\mathrm{Re}u_1(x,\omega_k)) = \int_D \Big[G_{\mathrm{Re}}^{[11]}(x,y,\omega_k)g_1(y) + G_{\mathrm{Re}}^{[12]}(x,y,\omega_k)g_2(y)\Big]\mathrm{d}y, \tag{3.4}$$

$$\mathbf{E}(\mathrm{Re}u_2(x,\omega_k)) = \int_D \Big[G_{\mathrm{Re}}^{[21]}(x,y,\omega_k)g_1(y) + G_{\mathrm{Re}}^{[22]}(x,y,\omega_k)g_2(y)\Big]\mathrm{d}y, \tag{3.5}$$

$$\mathbf{E}(\mathrm{Im}u_1(x,\omega_k)) = \int_D \Big[G_{\mathrm{Im}}^{[11]}(x,y,\omega_k)g_1(y) + G_{\mathrm{Im}}^{[12]}(x,y,\omega_k)g_2(y)\Big]\mathrm{d}y, \tag{3.6}$$

$$\mathbf{E}(\mathrm{Im}u_2(x,\omega_k)) = \int_D \Big[G_{\mathrm{Im}}^{[21]}(x,y,\omega_k)g_1(y) + G_{\mathrm{Im}}^{[22]}(x,y,\omega_k)g_2(y)\Big]\mathrm{d}y. \tag{3.7}$$

It is known that Fredholm integral equations of the first kind are ill-posed due to the rapidly decaying singular values of matrices from the discretized integral kernels. Appropriate regularization methods are needed to recover the information about the solutions as stably as possible. As a representative example, Figure 3.1 plots the singular values of the matrices for the Fredholm integral equations (3.4)–(3.7) at $\omega = 1.9\pi$. We can observe similar decaying patterns for the singular values of (3.4) and (3.6) for the component u_1, and of (3.5) and (3.7) for the component u_2.

To reconstruct the variance $\boldsymbol{h}^2$, we use Proposition A.3 to obtain

$$\begin{aligned}
&\mathbf{E}\Big(\Big|\int_D \mathrm{Re}\mathbb{G}(x,y,\omega_k)\boldsymbol{h}(y)\mathrm{d}W_y\Big|^2\Big) = \int_D \|\mathrm{Re}\mathbb{G}(x,y,\omega_k)\boldsymbol{h}(y)\|^2\mathrm{d}y\\
&= \int_D \Big[(G_{\mathrm{Re}}^{[11]}(x,y,\omega_k))^2 + (G_{\mathrm{Re}}^{[21]}(x,y,\omega_k))^2\Big]h_1^2(y)\mathrm{d}y\\
&\quad + \int_D \Big[(G_{\mathrm{Re}}^{[12]}(x,y,\omega_k))^2 + (G_{\mathrm{Re}}^{[22]}(x,y,\omega_k))^2\Big]h_2^2(y)\mathrm{d}y
\end{aligned}$$

and

$$\begin{aligned}
&\mathbf{E}\Big(\Big|\int_D \mathrm{Im}\mathbb{G}(x,y,\omega_k)\boldsymbol{h}(y)\mathrm{d}W_y\Big|^2\Big) = \int_D \|\mathrm{Im}\mathbb{G}(x,y,\omega_k)\boldsymbol{h}(y)\|^2\mathrm{d}y\\
&= \int_D \Big[(G_{\mathrm{Im}}^{[11]}(x,y,\omega_k))^2 + (G_{\mathrm{Im}}^{[21]}(x,y,\omega_k))^2\Big]h_1^2(y)\mathrm{d}y\\
&\quad + \int_D \Big[(G_{\mathrm{Im}}^{[12]}(x,y,\omega_k))^2 + (G_{\mathrm{Im}}^{[22]}(x,y,\omega_k))^2\Big]h_2^2(y)\mathrm{d}y.
\end{aligned}$$

Taking the variance on both sides of (3.2) and (3.3), we get

$$\begin{aligned}\mathbf{V}(\mathrm{Re}\boldsymbol{u}(x,\omega_k)) &= \int_D \Big[(G^{[11]}_{\mathrm{Re}}(x,y,\omega_k))^2 + (G^{[21]}_{\mathrm{Re}}(x,y,\omega_k))^2\Big]h_1^2(y)\mathrm{d}y \\ &\quad + \int_D \Big[(G^{[12]}_{\mathrm{Re}}(x,y,\omega_k))^2 + (G^{[22]}_{\mathrm{Re}}(x,y,\omega_k))^2\Big]h_2^2(y)\mathrm{d}y, \\ \mathbf{V}(\mathrm{Im}\boldsymbol{u}(x,\omega_k)) &= \int_D \Big[(G^{[11]}_{\mathrm{Im}}(x,y,\omega_k))^2 + (G^{[21]}_{\mathrm{Im}}(x,y,\omega_k))^2\Big]h_1^2(y)\mathrm{d}y \\ &\quad + \int_D \Big[(G^{[12]}_{\mathrm{Im}}(x,y,\omega_k))^2 + (G^{[22]}_{\mathrm{Im}}(x,y,\omega_k))^2\Big]h_2^2(y)\mathrm{d}y,\end{aligned}$$

which are the Fredholm integral equations of the first kind to reconstruct the variance. Again, we consider the variance of components u_1 and u_2:

$$\mathbf{V}(\mathrm{Re}u_1(x,\omega_k)) = \int_D \Big[\big(G^{[11]}_{\mathrm{Re}}(x,y,\omega_k)\big)^2 h_1^2(y) + \big(G^{[12]}_{\mathrm{Re}}(x,y,\omega_k)\big)^2 h_2^2(y)\Big]\mathrm{d}y, \tag{3.8}$$

$$\mathbf{V}(\mathrm{Re}u_2(x,\omega_k)) = \int_D \Big[\big(G^{[21]}_{\mathrm{Re}}(x,y,\omega_k)\big)^2 h_1^2(y) + \big(G^{[22]}_{\mathrm{Re}}(x,y,\omega_k)\big)^2 h_2^2(y)\Big]\mathrm{d}y, \tag{3.9}$$

$$\mathbf{V}(\mathrm{Im}u_1(x,\omega_k)) = \int_D \Big[\big(G^{[11]}_{\mathrm{Im}}(x,y,\omega_k)\big)^2 h_1^2(y) + \big(G^{[12]}_{\mathrm{Im}}(x,y,\omega_k)\big)^2 h_2^2(y)\Big]\mathrm{d}y, \tag{3.10}$$

$$\mathbf{V}(\mathrm{Im}u_2(x,\omega_k)) = \int_D \Big[\big(G^{[21]}_{\mathrm{Im}}(x,y,\omega_k)\big)^2 h_1^2(y) + \big(G^{[22]}_{\mathrm{Im}}(x,y,\omega_k)\big)^2 h_2^2(y)\Big]\mathrm{d}y. \tag{3.11}$$

To investigate ill-posedness of the above four equations, we plot their singular values in Figure 3.2. It can be seen that (3.8), (3.10) and (3.9), (3.11) show almost identical distributions of the singular values for components u_1 and u_2, respectively. The singular values decay exponentially to zeros and there is a big gap between the few leading singular values and the rests. Hence it is severely ill-posed to use directly either (3.8) or (3.10) and (3.9) or (3.11) to reconstruct h_1^2 and h_2^2. Subtracting (3.10) from (3.8) and (3.11) from (3.9), we obtain the improved equations to reconstruct h_1^2 and h_2^2:

$$\begin{aligned}\mathbf{V}(\mathrm{Re}u_1(x,\omega_k)) - \mathbf{V}(\mathrm{Im}u_1(x,\omega_k)) &= \int_D \Big[\big(G^{[11]}_{\mathrm{Re}}(x,y,\omega_k)\big)^2 - \big(G^{[11]}_{\mathrm{Im}}(x,y,\omega_k)\big)^2\Big]h_1^2(y)\mathrm{d}y \\ &\quad + \int_D \Big[\big(G^{[12]}_{\mathrm{Re}}(x,y,\omega_k)\big)^2 - \big(G^{[12]}_{\mathrm{Im}}(x,y,\omega_k)\big)^2\Big]h_2^2(y)\mathrm{d}y, \qquad (3.12)\end{aligned}$$

$$\begin{aligned}\mathbf{V}(\mathrm{Re}u_2(x,\omega_k)) - \mathbf{V}(\mathrm{Im}u_2(x,\omega_k)) &= \int_D \Big[\big(G^{[21]}_{\mathrm{Re}}(x,y,\omega_k)\big)^2 - \big(G^{[21]}_{\mathrm{Im}}(x,y,\omega_k)\big)^2\Big]h_1^2(y)\mathrm{d}y \\ &\quad + \int_D \Big[\big(G^{[22]}_{\mathrm{Re}}(x,y,\omega_k)\big)^2 - \big(G^{[22]}_{\mathrm{Im}}(x,y,\omega_k)\big)^2\Big]h_2^2(y)\mathrm{d}y. \qquad (3.13)\end{aligned}$$

In fact, it is clear to note in Figure 3.2 that the singular values of (3.12) and (3.13) display better behavior that those of (3.8), (3.10) and (3.9), (3.11). The singular values decay more slowly and distribute more uniformly. Numerically, (3.12) and (3.13) do give much better reconstructions. We will only show the results for (3.12) and (3.13) in the numerical experiments.

3.2. Numerical method. In this section, we present a regularized Kaczmarz method to solve the ill-posed integral equations. The classical Kaczmarz method is an iterative method for solving linear systems of algebraic equations [30].

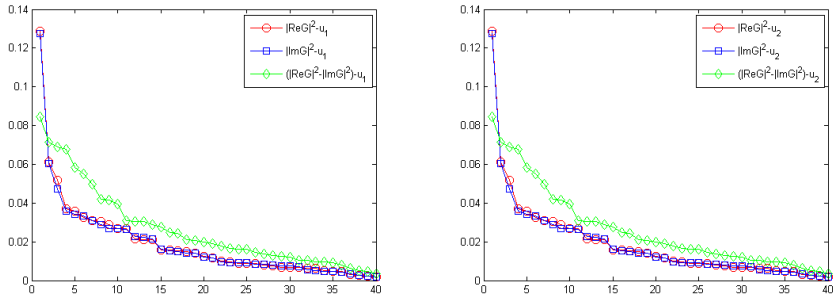

FIG. 3.2. *Singular values of the Fredholm integral equations for the reconstruction of* $\boldsymbol{h}^2$*: (left) component of* u_1*; (right) component of* u_2*.*

Consider the following operator equations

$$A_k q = p_k, \quad k = 1, \ldots, K, \tag{3.14}$$

where the index k is for different frequency, q represents the unknown g_1, g_2 or h_1^2, h_2^2, and p_k is the given data. Given an arbitrary initial guess q^0, the classical Kaczmarz method for solving (3.14) reads: For $l = 0, 1, \ldots, L$,

$$\begin{cases} q_0 = q^l, \\ q_k = q_{k-1} + A_k^*(A_k A_k^*)^{-1}(p_k - A_k q_{k-1}), \quad k = 1, \ldots, K, \\ q^{l+1} = q_K, \end{cases} \tag{3.15}$$

where A_k^* is the adjoint operator of A_k. In (3.15), there are two loops: the outer loop is carried for iterative index l and the inner loop is done for the different frequency ω_k. In practice, the operator $A_k A_k^*$ may not be invertible or is bad conditioned even if it is invertible. A regularization technique is needed.

We present a regularized Kaczmarz method: Given an arbitrary initial guess q^0,

$$\begin{cases} q_0 = q^l, \\ q_k = q_{k-1} + A_k^*(\gamma I + A_k A_k^*)^{-1}(p_k - A_k q_{k-1}), \quad k = 1, \ldots, K, \\ q^{l+1} = q_m, \end{cases} \tag{3.16}$$

for $l = 0, 1, \ldots, L$, where $\gamma > 0$ is the regularization parameter and I is the identity operator. Although there are two loops in (3.16), the operator $\gamma I + A_k A_k^*$ leads to a small scale linear system of equations with the size equal to the number of measurements. Moreover, they essentially need to be solved only K times by a direct solver such as the LU decomposition since A_k keep the same during the outer loop.

4. Numerical experiments. In this section, we present a numerical example to demonstrate the validity and effectiveness of the proposed method. The scattering data is obtained by the numerical solution of the stochastic Navier equation instead of the numerical integration of the Fredholm integral equations in order to avoid the so-called inverse crime. Although the stochastic Navier equation may be efficiently solved by using the Wiener Chaos expansions to obtain statistical moments such as the mean and variance [4], we choose the Monte Carlo method to simulate the actual process of measuring data. In each realization, the stochastic Navier equation is solved

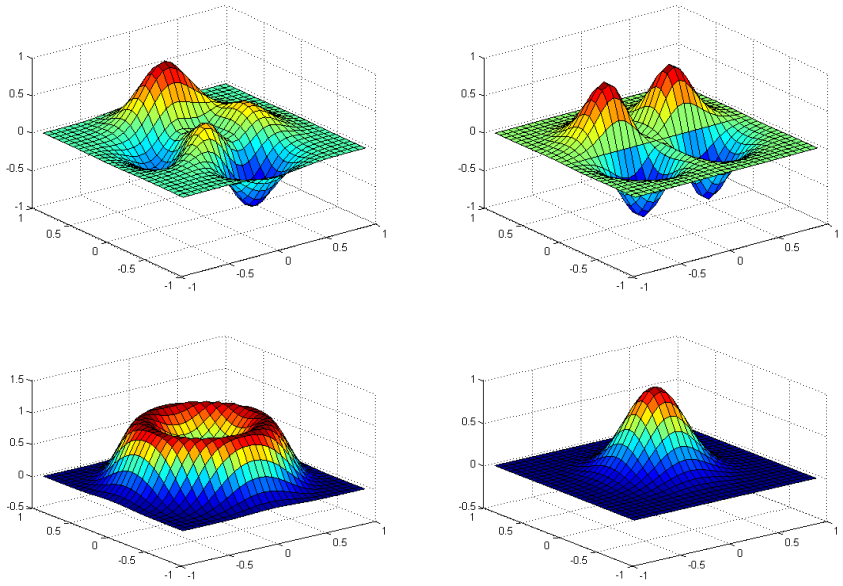

FIG. 4.1. *The exact source: (top) surface plot of the exact mean g_1 and g_2; (below) surface plot of the exact variance h_1^2 and h_2^2.*

by using the finite element method with the perfectly matched layer (PML) technique. After all the realizations are done, we take an average of the solutions and use it as an approximated scattering data to either the mean or the variance. It is clear to note that the data is more accurate as more number of realizations is taken.

Let

$$g_1(x_1,x_2) = 0.3(1-x_1)^2 e^{-x_1^2-(x_2+1)^2} - (0.2x_1 - x_1^3 - x_2^5)e^{-x_1^2-x_2^2} - 0.03e^{-(x_1+1)^2-x_2^2}$$

and

$$g_2(x_1,x_2) = 5x_1^2 x_2 e^{-x_1^2-x_2^2}.$$

We reconstruct the mean $\boldsymbol{g}$ given by

$$\boldsymbol{g}(x_1,x_2) = (g_1(3x_1,3x_2), g_2(3x_1,3x_2))^\top$$

inside the domain $D = [-1,\,1]\times[-1,\,1]$. Let

$$h_1(x_1,x_2) = 0.6e^{-8(r^3-0.75r^2)}$$

and

$$h_2(x_1,x_2) = e^{-r^2}, \quad r = (x_1^2+x_2^2)^{1/2}.$$

We reconstruct the variance $\boldsymbol{h}^2$ given by

$$\boldsymbol{h}^2(x_1,x_2) = \begin{bmatrix} h_1^2(x_1,x_2) & 0 \\ 0 & h_2^2(3x_1,3x_2) \end{bmatrix}$$

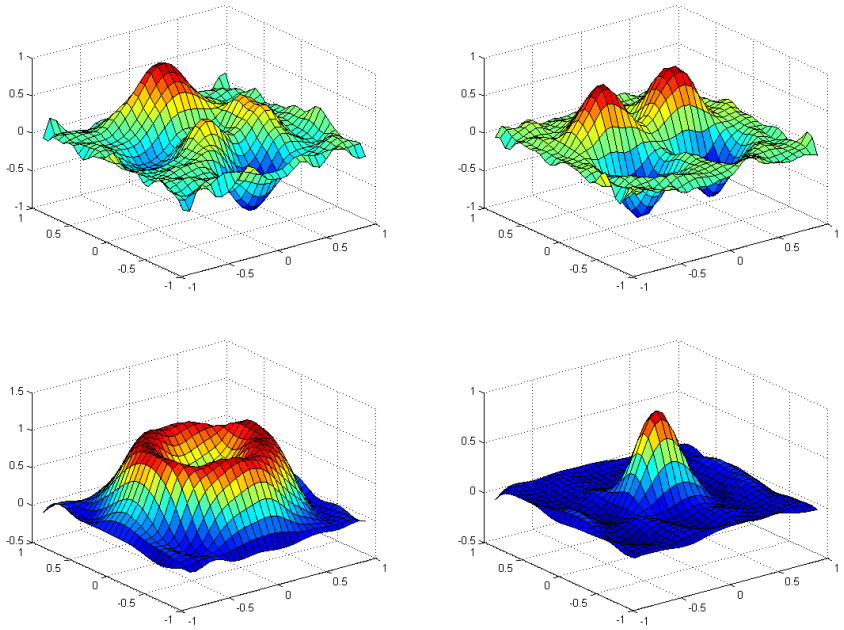

FIG. 4.2. *The reconstructed source: (top) surface plot of the reconstructed mean g_1, g_2; (below) surface plot of the reconstructed variance h_1^2, h_2^2.*

inside the domain $D = [-1, 1]\times[-1, 1]$. See Figure 4.1 for the surface plot of the exact g_1, g_2 (top) and h_1^2, h_2^2 (below). The Lamé constants are $\mu = 1.0$ and $\lambda = 2.0$. The computational domain is set to be $[-3, 3]\times[-3, 3]$ with the PML thickness 0.5. After the direct problem is solved and the value of $\boldsymbol{u}$ is obtained at the grid points, the linear interpolation is used to generate the synthetic data at 40 uniformly distributed points on the circle with radius 2, i.e., $x_1 = 2\cos\theta_i, x_2 = 2\sin\theta_i, \theta_i = i\pi/20, i = 0, 1, \ldots, 39$. Sixteen equally spaced frequencies from 0.5π to 7.5π are used in the reconstruction of g_1, g_2, while twenty equally spaced frequencies from 0.5π to 2.5π are used in the reconstruction of h_1^2, h_2^2. The regularization parameter is $\gamma = 1.0 \times 10^{-7}$ and the total number of the outer loop for the Kaczmarz method is $L = 5$. Figure 4.2 shows the reconstructed mean g_1, g_2 (top) and the reconstructed variance h_1^2, h_2^2 (below) corresponding to the number of realization 10^4.

5. Conclusion. We have studied the direct and inverse random source scattering problems for the stochastic Navier equation where the source is driven by an additive white noise. Under a suitable regularity assumption of the source functions $\boldsymbol{g}$ and $\boldsymbol{h}$, the direct scattering problem is shown constructively to have a unique mild solution which was given explicitly as an integral equation. Based on the explicit solution, Fredholm integral equations are deduced for the inverse scattering problem to reconstruct the mean and the variance of the random source. We have presented the regularized Kaczmarz method to solve the ill-posed integral equations by using multiple frequency data. A numerical example is presented to demonstrate the validity and effectiveness of the proposed method. We are currently investigating the inverse random source scattering problem in an inhomogeneous elastic medium where the explicit Green tensor function is no longer available. Although this paper concerns

the inverse random source scattering problem for the Navier equation, we believe that the proposed framework and methodology can be directly applied to solve many other inverse random source problems and even more general stochastic inverse problems. For instance, it is interesting to study inverse random source problems for the stochastic Poisson, heat, or electromagnetic wave equation. Obviously, it is more challenging to consider the inverse random medium scattering problem where the medium should be modeled as a random function. We hope to be able to report the progress on these problems in the future.

Appendix A. Brownian sheet.

Let us first briefly introduce the one-dimensional Brownian sheet, which is also called one-dimensional d-parameter Brownian motion, on $(\mathbb{R}^d_+, \mathcal{B}(\mathbb{R}^d_+), \mu)$, where $d \in \mathbb{N}, \mathbb{R}^d_+ = \{x = (x_1, \ldots, x_d)^\top \in \mathbb{R}^d : x_j \geq 0, j = 1, \ldots, d\}$, $\mathcal{B}(\mathbb{R}^d_+)$ is the Borel σ-algebra of $\mathbb{R}^d_+$, and μ is the Lebesgue measure. More details can be found in [31]. Let $(0, x] = (0, x_1] \times \cdots \times (0, x_d]$ for $x \in \mathbb{R}^d_+$.

DEFINITION A.1. *The one-dimensional Brownian sheet on $\mathbb{R}^d_+$ is the process $\{W_x : x \in \mathbb{R}^d_+\}$ defined by $W_x = W\{(0, x]\}$, where W is a random set function such that*

1. *$\forall A \in \mathcal{B}(\mathbb{R}^d_+)$, $W(A)$ is a Gaussian random variable with mean 0 and variance $\mu(A)$, i.e., $W(A) \sim \mathcal{N}(0, \mu(A))$;*
2. *$\forall A, B \in \mathcal{B}(\mathbb{R}^d_+)$, if $A \cap B = \emptyset$, then $W(A)$ and $W(B)$ are independent and $W(A \cup B) = W(A) + W(B)$.*

It can be verified from Definition A.1 that

$$\mathbf{E}(W(A)W(B)) = \mu(A \cap B), \quad \forall A, B \in \mathcal{B}(\mathbb{R}^d_+),$$

which gives the covariance function of the Brownian sheet:

$$\mathbf{E}(W_x W_y) = x \wedge y := (x_1 \wedge y_1) \cdots (x_d \wedge y_d)$$

for any $x = (x_1, \ldots, x_d)^\top \in \mathbb{R}^d_+$ and $y = (y_1, \ldots, y_d)^\top \in \mathbb{R}^d_+$, where $x_j \wedge y_j = \min\{x_j, y_j\}$.

The Brownian sheet can be generalized to the space $\mathbb{R}^d$ by introducing 2^d independent Brownian sheets defined on $\mathbb{R}^d_+$. Define a multi-index $t = (t_1, \ldots, t_d)^\top$ with $t_j = \{1, -1\}$ for $j = 1, \ldots, d$. Introduce 2^d independent Brownian sheets $\{W^t\}$ defined on $\mathbb{R}^d_+$. For any $x = (x_1, \ldots, x_d)^\top \in \mathbb{R}^d$, define the Brownian sheet

$$W_x := W^{t(x)}_{\breve{x}},$$

where $\breve{x} = (|x_1|, \ldots, |x_d|)^\top$ and $t(x) = (\mathrm{sgn}(x_1), \ldots, \mathrm{sgn}(x_d))^\top$. The sign function $\mathrm{sgn}(x_j) = 1$ if $x_j \geq 0$, otherwise $\mathrm{sgn}(x_j) = -1$.

In two or more parameters, the white noise can be thought of as the derivative of the Brownian sheet. In fact, the Brownian sheet W_x is nowhere-differentiable in the ordinary sense, but its derivatives will exist in the sense of Schwartz distributions. Define

$$\dot{W}_x = \frac{\partial^d W_x}{\partial x_1 \cdots \partial x_d}.$$

If $\phi(x)$ is a deterministic square-integrable complex-valued test function with a compact support in $\mathbb{R}^d$, then $\dot{W}_x$ is the distribution

$$\dot{W}_x(\phi) = (-1)^d \int_{\mathbb{R}^d} W_x \frac{\partial^d \phi(x)}{\partial x_1 \cdots \partial x_d} \mathrm{d}x.$$

We may define the stochastic integral

$$\int_{\mathbb{R}^d} \phi(x)\mathrm{d}W_x = (-1)^d \int_{\mathbb{R}^d} W_x \frac{\partial^d \phi(x)}{\partial x_1 \cdots \partial x_d}\mathrm{d}x, \tag{A.1}$$

which satisfies the following properties (cf. [5, Proposition A.2]).

LEMMA A.2. *Let $\phi(x)$ be a test function with a compact support in $\mathbb{R}^d$. We have*

$$\mathbf{E}\Big(\int_{\mathbb{R}^d} \phi(x)\mathrm{d}W_x\Big) = 0, \quad \mathbf{E}\Big(\big|\int_{\mathbb{R}^d} \phi(x)\mathrm{d}W_x\big|^2\Big) = \int_{\mathbb{R}^d} |\phi(x)|^2\mathrm{d}x.$$

The stochastic integral (A.1) can be extended to define the multi-dimensional stochastic integrals. Let $W(x) = (W_1(x), \ldots, W_n(x))^\top$ be an n-dimensional Brownian sheet, where $W_i(x)$ and $W_j(x)$ are two one-dimensional independent Brownian sheets for $i \neq j$. If $\phi(x)$ is a deterministic square-integrable complex-valued $m \times n$ matrix-valued test function with each component compactly supported in $\mathbb{R}^d$, i.e.,

$$\phi(x) = \begin{bmatrix} \phi_{11}(x) & \cdots & \phi_{1n}(x) \\ \vdots & & \vdots \\ \phi_{m1}(x) & \cdots & \phi_{mn}(x) \end{bmatrix}.$$

Using the matrix notation, we may define the multi-dimensional stochastic integral

$$\int_{\mathbb{R}^d} \phi(x)\mathrm{d}W(x) = \int_{\mathbb{R}^d} \begin{bmatrix} \phi_{11}(x) & \cdots & \phi_{1n}(x) \\ \vdots & & \vdots \\ \phi_{m1}(x) & \cdots & \phi_{mn}(x) \end{bmatrix} \begin{bmatrix} \mathrm{d}W_1(x) \\ \vdots \\ \mathrm{d}W_n(x) \end{bmatrix}, \tag{A.2}$$

which is an $m \times 1$ matrix and its j-th component is the sum of 1-dimensional stochastic integrals

$$\sum_{k=1}^{n} \int_{\mathbb{R}^d} \phi_{jk}(x)\mathrm{d}W_k(x).$$

We have the similar properties for the multi-dimensional stochastic integral.

PROPOSITION A.3. *Let $W(x) = (W_1(x), \ldots, W_n(x))^\top$ be an n-dimensional Brownian sheet and $\phi(x) = (\phi_{ij}(x))_{m\times n}$ be an $m \times n$ matrix-valued function with each component $\phi_{ij}(x)$ compactly supported in $\mathbb{R}^d$. We have*

$$\mathbf{E}\Big(\int_{\mathbb{R}^d} \phi(x)\mathrm{d}W_x\Big) = 0, \quad \mathbf{E}\Big(\big|\int_{\mathbb{R}^d} \phi(x)\mathrm{d}W_x\big|^2\Big) = \int_{\mathbb{R}^d} \|\phi(x)\|^2\mathrm{d}x,$$

where $\|\cdot\|$ is the Frobenius norm.

Proof. It follows from (A.2) and Lemma A.2 that

$$\mathbf{E}\Big(\int_{\mathbb{R}^d} \phi(x)\mathrm{d}W_x\Big) = \begin{bmatrix} \sum_{k=1}^n \mathbf{E}\Big(\int_{\mathbb{R}^d} \phi_{jk}(x)\mathrm{d}W_k(x)\Big) \\ \vdots \\ \sum_{k=1}^n \mathbf{E}\Big(\int_{\mathbb{R}^d} \phi_{jk}(x)\mathrm{d}W_k(x)\Big) \end{bmatrix} = 0.$$

Using (A.2) and Lemma A.2 again, we have

$$\begin{aligned}\mathbf{E}\Big(\Big|\int_{\mathbb{R}^d}\phi(x)\mathrm{d}W_x\Big|^2\Big) &= \sum_{j=1}^m \mathbf{E}\Big(\Big|\sum_{k=1}^n\int_{\mathbb{R}^d}\phi_{jk}(x)\mathrm{d}W_k(x)\Big|^2\Big)\\ &= \sum_{j=1}^m\sum_{k=1}^n\int_{\mathbb{R}^d}|\phi_{jk}(x)|^2\mathrm{d}x\\ &= \int_{\mathbb{R}^d}\|\phi(x)\|^2\mathrm{d}x,\end{aligned}$$

which completes the proof. □

REFERENCES

[1] R. Albanese and P. Monk, The inverse source problem for Maxwell's equations, Inverse Problems, 22 (2006), 1023–1035.

[2] H. Ammari, G. Bao, and J. Fleming, An inverse source problem for Maxwell's equations in magnetoencephalography, SIAM J. Appl. Math., 62 (2002), 1369–1382.

[3] A. Badia and T. Nara, An inverse source problem for Helmholtz's equation from the Cauchy data with a single wave number, Inverse Problems, 27 (2011), 105001.

[4] M. Badieirostami, A. Adibi, H.-M. Zhou, and S.-N. Chow, Wiener chaos expansion and simulation of electromagnetic wave propagation excited by a spatially incoherent source, Multiscale Model. Simul., 8 (2010), pp. 591–604.

[5] G. Bao, C. Chen and P. Li, Inverse random source scattering problems in several dimensions, preprint.

[6] G. Bao, S.-N. Chow, P. Li, and H.-M. Zhou, An inverse random source problem for the Helmholtz equation, Math. Comp., 83 (2014), 215–233.

[7] G. Bao, P. Li, J. Lin, and F. Triki, Inverse scattering problems with multi-frequencies, Inverse Problems, 31 (2015), 093001.

[8] G. Bao, J. Lin, and F. Triki, A multi-frequency inverse source problem, J. Differential Equations, 249 (2010), 3443–3465.

[9] G. Bao, S. Lu, W. Rundell, and B. Xu, A recursive algorithm for multifrequency acoustic inverse source problems, SIAM J. Numer. Anal., 53 (2015), 1608–1628.

[10] G. Bao and X. Xu, An inverse random source problem in quantifying the elastic modulus of nano-materials, Inverse Problems, 29 (2013), 015006.

[11] M. Bonnet and A. Constantinescu, Inverse problems in elasticity, Inverse Problems, 21 (2005) 1–50,

[12] Y.-Z. Cao, R. Zhang, and K. Zhang, Finite element method and discontinuous Galerkin method for stochastic Helmholtz equation in two- and three-dimensions, J. Comput. Math., 26 (2008), 701–715.

[13] D. Colton and R. Kress, Inverse Acoustic and Electromagnetic Scattering Theory, Berlin: Springer, 1998.

[14] A. Devaney, The inverse problem for random sources, J. Math. Phys., 20 (1979), 1687–1691.

[15] A. Devaney, E. Marengo, and M. Li, Inverse source problem in nonhomogeneous background media, SIAM J. Appl. Math., 67 (2007), 1353–1378.

[16] A. Devaney and G. Sherman, Nonuniqueness in inverse source and scattering problems, IEEE Trans. Antennas Propag., 30 (1982), 1034–1037.

[17] M. Eller and N. Valdivia, Acoustic source identification using multiple frequency information, Inverse Problems, 25 (2009), 115005.

[18] L. Evans, An Introduction to Stochastic Differential Equations, AMS, 2013.

[19] A. Fokas, Y. Kurylev, and V. Marinakis, The unique determination of neuronal currents in the brain via magnetoencephalogrphy, Inverse Problems, 20 (2004), 1067–1082.

[20] A. Friedman, Stochastic Differential Equations and Applications, New York: Academic Press, 2006.

[21] K.-H. Hauer, L. Kühn, and R. Potthast, On uniqueness and non-uniqueness for current reconstruction from magnetic fields, Inverse Problems, 21 (2005), 955–967.

[22] M. Hairer, Introduction to Stochastic PDEs, lecture notes, 2009.

[23] V. Isakov, Inverse Source Problems, AMS, Providence, RI, 1989.

[24] J. Kaipio and E. Somersalo, Statistical and Computational Inverse Problems, Springer-Varlag, New York, 2005.
[25] R. Kress, Inverse elastic scattering from a crack, Inverse Problems, 12 (1996), 667–684.
[26] L. D. Landau and E. M. Lifshitz, Theory of Elasticity, Oxford, UK: Pergamon, 1986.
[27] P. Li, An inverse random source scattering problem in inhomogeneous media, Inverse Problems, 27 (2011), 035004.
[28] P. Li, Y. Wang, and Y. Zhao, Inverse elastic surface scattering with near-field data, Inverse Problems, 31 (2015), 035009.
[29] E. Marengo and A. Devaney, The inverse source problem of electromagnetics: linear inversion formulation and minimum energy solution, IEEE Trans. Antennas Propag., 47 (1999), 410–412.
[30] F. Natterer, The Mathematics of Computerized Tomography, Teubner, Stuttgart, 1986.
[31] J. Walsh, An Introduction to Stochastic Partial Differential Equations, Springer, 1986.
[32] D. Zhang and Y. Guo, Fourier method for solving the multi-frequency inverse acoustic source problem for the Helmholtz equation, Inverse Problems, 31 (2015), 035007.